

AD

AD 708868

TECHNICAL REPORT

WVT-7026

A COMPLIANCE K CALIBRATION FOR A PRESSURIZED
THICK-WALL CYLINDER WITH A RADIAL CRACK

BY

JOHN H. UNDERWOOD

RALPH R. LASSELLE

RAYMOND D. SCANLON

AND

MOAYYED A. HUSSAIN

This document has been approved
for public release and sale; its
distribution is unlimited.

MAY 1970

BENET R&E LABORATORIES

WATERVLIET ARSENAL

WATERVLIET-NEW YORK

AWGNS No. 5010.11.85500

DA Project No. 17001102032A

WATERVLIET
CLEARINGHOUSE
17001102032A
Introduction, Summary, etc.

DDC
RECEIVED
JUL 22 1970
C

34

A COMPLIANCE K CALIBRATION FOR A PRESSURIZED THICK-WALL CYLINDER WITH A RADIAL CRACK

Abstract

The K calibration for an internally pressurized, thick-wall cylinder with a straight, radial notch has been determined from a compliance test. The method suggested by Irwin is used with compliance defined as the change in internal volume of a cylinder divided by applied hydrostatic pressure rather than the usual load-elongation definition. The derivative of internal volume change with respect to notch depth, "a", is obtained by numerical analysis of tangential strain measurements on the OD of the test cylinder. This derivative leads directly to the K calibration for the cylinder. Cubic spline functions are used to approximate both the strain as a function of position on the cylinder and the resulting volume change as a function of "a". Also included in the determination of K is a proof, using the divergence theorem in the theory of elasticity, that the derivatives with respect to "a" of internal and external volume change are identical. This allows the use of external strain measurements to determine K based on internal volume change.

The compliance K calibration nearly coincides with a semi-infinite plate solution simulating both the tangential stress due to pressure and the direct effect of pressure in the notch, $K_I = 1.12 \sigma_0 \sqrt{\pi a} + 1.13 p \sqrt{\pi a}$. This unexpected agreement, particularly for values of a/w up to 0.6, is explained by the combination of bending constraint and drop off of tangential stress in the cylinder wall.

Cross-Reference Data

Fracture
Mechanics
Stress Intensity
Factor
Compliance
Test
Cubic Spline
Functions
Divergence
Theorem

TABLE OF CONTENTS

	Page
Abstract	1
Notation	4
Acknowledgments	5
Introduction	6
Fracture Mechanics Analysis	6
Compliance Test	12
Numerical Data Analysis	16
Results and Discussion	21
References	30
DD Form 1473 (Document Control Data - R&D)	

Figures

1. Cylinder Geometry	9
2. Compliance Test Set-up	13
3. Measured Strain Distribution	15
4. Numerical Strain Data	19
5. Compliance K Calibration Results	22
6. Variation of K with h	24
7. K Results from Experiment and Analysis	25
8. Comparison of K Results	28

Tables

	Page
I. Measured Tangential Strain at 10,000 psi Pressure	14
II. Change in Area Enclosed by the Outside Perimeter of the Cylinder	20

NOTATION

- a - Crack or notch depth
- A - Cross-section area of cylinder material
- A_0 - Area enclosed by the outside perimeter of the cylinder
- C - Compliance, change in length divided by load for a unit thickness sheet
- C_v - Compliance, internal volume change divided by pressure for a unit length cylinder
- E - Young's modulus
- G - Crack extension force per unit length along the crack front
- h - Constant applied to plastic zone correction
- K_I - Opening mode stress intensity factor
- p - Hydrostatic pressure on the ID of a cylinder
- r - Radial coordinate of a cylinder
- r_1 - Inner radius of a cylinder
- r_2 - Outer radius of a cylinder
- V_i - Volume enclosed by the inner surface of a unit length cylinder
- V_m - Material volume of a unit length cylinder
- V_o - Volume enclosed by the outer surface of a unit length cylinder
- w - Wall thickness of a cylinder
- z - Length coordinate of a cylinder
- σ - Uniform tensile stress
- σ_θ - Tangential stress in a cylinder wall
- σ_y - Tensile yield stress, 0.2%

Other notation defined in the text.

ACKNOWLEDGMENTS

The authors gratefully acknowledge the help of Mr. James Delaney in performing the experiment and Miss Sheila Peach in analyzing the data. We also thank Messrs. Joseph Throop and David Kendall for their helpful discussions during the course of this work.

INTRODUCTION

The determination of stress intensity factors by an experimental compliance test is seldom reported in the literature. This is probably due to the difficulty in performing compliance experiments with sufficient accuracy and also due to the limited application of the experimental results, once obtained. Numerical and analytical K calibrations are often at least as reliable and as easy to obtain. They can often be applied to many different geometries with little difficulty. However, experimental K calibrations can be useful when the geometry is difficult to model or when the experiment is relatively simple.

In this case the compliance testing of a pressurized thick-wall cylinder with a narrow radial notch was performed as part of another experiment. Our purpose here is to use the available compliance results to determine the K calibration of a thick-wall cylinder for use in design and for comparison with other fracture mechanics analyses. The analysis in the literature which appears closest to a thick-wall cylinder geometry is Bowie's solution for a pressurized hole with a radial crack in an infinite plate⁽¹⁾. His solution should correspond to a pressurized cylinder with a radial crack in an infinitely thick wall. The experimental results will be compared with this and other analyses in the sections that follow.

FRACTURE MECHANICS ANALYSIS

The compliance method used to determine the K calibration for a pressurized cylinder is patterned after Irwin's method⁽²⁾. The usual definition of

compliance, i.e., the ratio of change in length of a specimen to the applied load, is replaced by the ratio of change in internal volume of a cylinder to the applied pressure. Internal volume and pressure are used to obtain an expression for crack extension force for a pressurized cylinder similar to Irwin's expression for a load-displacement system from Ref. (2), which is:

$$G = \frac{1}{2} F^2 \frac{dC}{da} \quad (1)$$

where compliance, $C = \frac{\Delta l}{F}$, is in terms of the tensile load, F , on a specimen and the resulting change in length, Δl . In the above, G and C are written in terms of unit specimen thickness, i.e., unit dimension along the crack front.

For a unit length cylinder at constant internal pressure, the differential change in strain energy, U , corresponding to a change in internal volume can be written

$$dU = \frac{1}{2} p d(\Delta V_i)$$

The Griffith crack extension force is defined as the differential change in strain energy of a system due to a change in crack depth. Thus,

$$\frac{dU}{da} \equiv G = \frac{1}{2} p \frac{d(\Delta V_i)}{da}$$

Using a modified definition of compliance $C_v = \frac{\Delta V_i}{p}$ and with p constant, the crack extension force becomes

$$G = \frac{1}{2} p^2 \frac{dC_v}{da} \quad (2)$$

an expression analogous to eq. (1) with tensile load replaced by hydrostatic pressure. G and C_V are written in terms of unit dimension along the crack front as before, which in this case is in the length or z direction of the cylinder, see Fig. 1. For plane strain conditions, as in the compliance test described below, the stress intensity factor is

$$K_I^2 = \frac{E G}{1 - \nu^2} = \frac{E p^2}{2(1 - \nu^2)} \frac{d(\Delta V_I/p)}{da} \quad (3)$$

The K calibration can be calculated simply by determining the change in internal volume of the cylinder at a given value of pressure for a series of different notch depths and then performing the indicated differentiation. However, the measurement which can be easily made is the change in outside volume of the cylinder. If it can be shown that the derivative of compliance with respect to crack depth determined from the outside volume change is equivalent to that determined from the inside volume change, then the problem is solved. Rice⁽³⁾ has outlined an analysis which indicates that the derivatives are equivalent. In the complete analysis below we prove that the change in material volume of a cylinder is unaffected by the presence of the notch provided that tractions on the opposite sides of the notch are the same, and thus the two derivatives of compliance are equivalent.

The change in material volume in an elastic body is given by

$$\Delta V_m = \int_{V_m} e \, dV$$

For plane strain, the dilatation $e = \epsilon_{ii}$, $i = 1, 2$, hence

$$\Delta V_m/\text{unit length} = \int_A \epsilon_{ii} \, dA \quad (4)$$

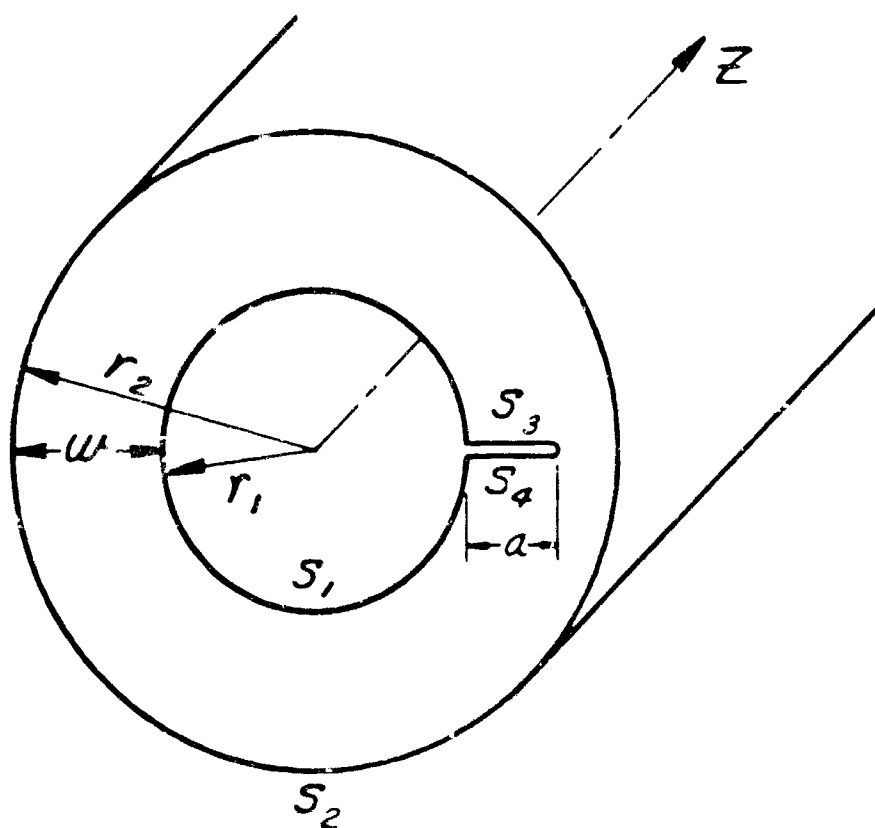


Figure 1. Cylinder Geometry

where A is the cross-section area of the body.

The stress-strain relations for plane-strain are

$$\epsilon_{ij} = \frac{1+\nu}{E} \tau_{ij} - \frac{\nu(1+\nu)}{E} \delta_{ij} \tau_{kk}$$

contraction gives

$$\epsilon_{ii} = \frac{(1+\nu)(1-2\nu)}{E} \tau_{ii} \quad (5)$$

Substituting (5) into (4) gives

$$\Delta V_m / \text{unit length} = \frac{(1+\nu)(1-2\nu)}{E} \int_A \tau_{ii} dA \quad (6)$$

The equation of equilibrium, in absence of body forces is

$$\tau_{ik,k} = 0 \quad i,k = 1,2$$

Now consider the following integral with the help of the above

$$\begin{aligned} \int_A \tau_{ij} dA &= \int_A \tau_{ik} \delta_{kj} dA + \int_A x_j \tau_{ik,k} dA \\ &= \int_A (\tau_{ik} x_{j,k} + x_j \tau_{ik,k}) dA \\ &= \int_A (\tau_{ik} x_j)_{,k} dA \end{aligned}$$

Using the divergence theorem we get the following line integral

$$\int_A (\tau_{ik} x_j)_{,k} dA = \int_S \nu_k \tau_{ik} x_j dS = \int_S \tilde{T}_1^j x_j dS$$

where ν_k are the direction cosines of the exterior normals $\underline{\nu}$ to the line S , and \underline{T}_i are the components of the tractions \underline{T} acting on S , see Ref. (4).

hence we have

$$\int_A \tau_{ij} dA = \int_S \underline{T}_i X_j dS$$

and contraction gives

$$\int_A \tau_{ii} dA = \int_S \underline{T}_i X_i dS = \int_S \underline{T} \cdot \underline{r} dS \quad (7)$$

Substituting (7) into (6) we have

$$\Delta V_m / \text{unit length} = \frac{(1 + \nu)(1 - 2\nu)}{E} \int_S \underline{T} \cdot \underline{r} dS$$

Breaking the line into four parts, $S = S_1 + S_2 + S_3 + S_4$, which correspond to the cylinder and notch surfaces as shown in Fig. 1, and keeping the outer normals in mind, we get

$$\begin{aligned} \Delta V_m / \text{unit length} = & \frac{(1 + \nu)(1 - 2\nu)}{E} \left\{ \oint_{S_1} \underline{T}_1 \cdot \underline{r} - \oint_{S_2} \underline{T}_2 \cdot \underline{r} \right\} \\ & - \frac{(1 + \nu)(1 - 2\nu)}{E} \left\{ \int_{r_1}^{r_1+a} \underline{T}_3 \cdot \underline{r} dS - \int_{r_1}^{r_1+a} \underline{T}_4 \cdot \underline{r} dS \right\} \quad (8) \end{aligned}$$

where $\underline{T}_1, \underline{T}_2$ are tractions on the inner and outer radii and $\underline{T}_3, \underline{T}_4$ are the tractions on the bottom and top of the notch. Now when $\underline{T}_3 = \underline{T}_4$, i.e., when the tractions on both sides of the notch are the same, the last two integrals vanish, and the proposition is proved. This is the case in the problem under consideration.

For our cylinder then, we have $\tilde{T}_1 = -e_r p$, $\tilde{T}_2 = 0$, where e_r is a unit vector in the radial direction. Using eq. (8) we get

$$\Delta V_m/\text{unit length} = \frac{(1+\nu)(1-2\nu)}{E} p r_1^2 2\pi,$$

the change in material volume of the cylinder per unit length in the z direction. This result can be checked directly from the Lamé solution (5).

From the above we have $\frac{\partial}{\partial a} (\Delta V_m/\text{unit length}) = 0$ so that eq. (3) can be written in terms of the outside volume, V_o , of the cylinder

$$K_I/p = \left[\frac{E}{2(1-\nu^2)} \frac{d(\Delta V_o/p)}{da} \right]^{1/2} \quad (9)$$

COMPLIANCE TEST

A 1.028 in. ID, 1.995 in. OD, 6 in. long, 4340 steel cylinder was pressure tested as shown in Fig. 2. The cylinder was tested in an open ended condition, i.e., the rams shown in the sketch served to carry the end loads due to the pressure as well as seal the ends of the cylinder. Thus, there were no z direction stresses produced in the cylinder due to pressure end-loads. The pressure fluid used was a synthetic instrument oil. No attempt was made to seal the notch area, so effects due to pressure in the crack were present in the tube.

The pressure was applied in four 10,000 psi increments for each of ten notch depths from 0 to .316 inches. The .015 in. thick, 4 in. long notch was cut deeper following each pressure run by an electrical discharge machining process. The circumferential strain on the OD of the cylinder was measured at the center of notch length with 16 resistance strain gages around the tube. The strain gage data for 10,000 psi pressure are listed in Table I.

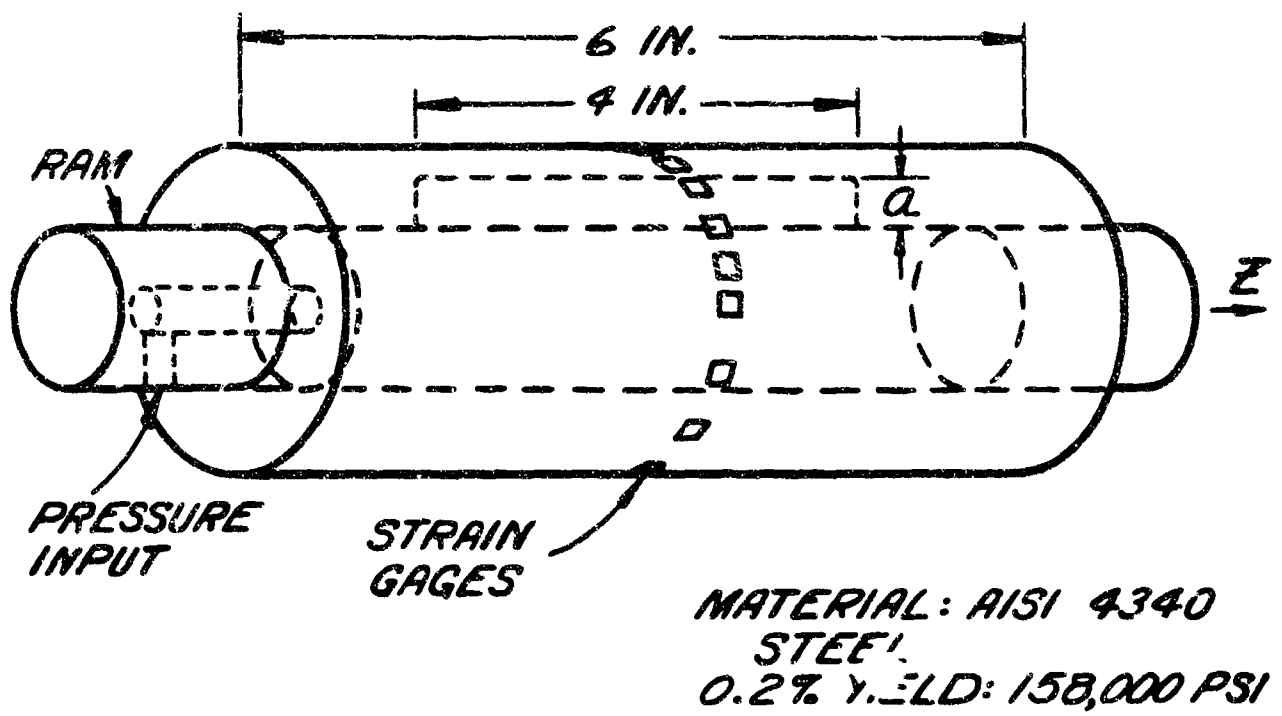


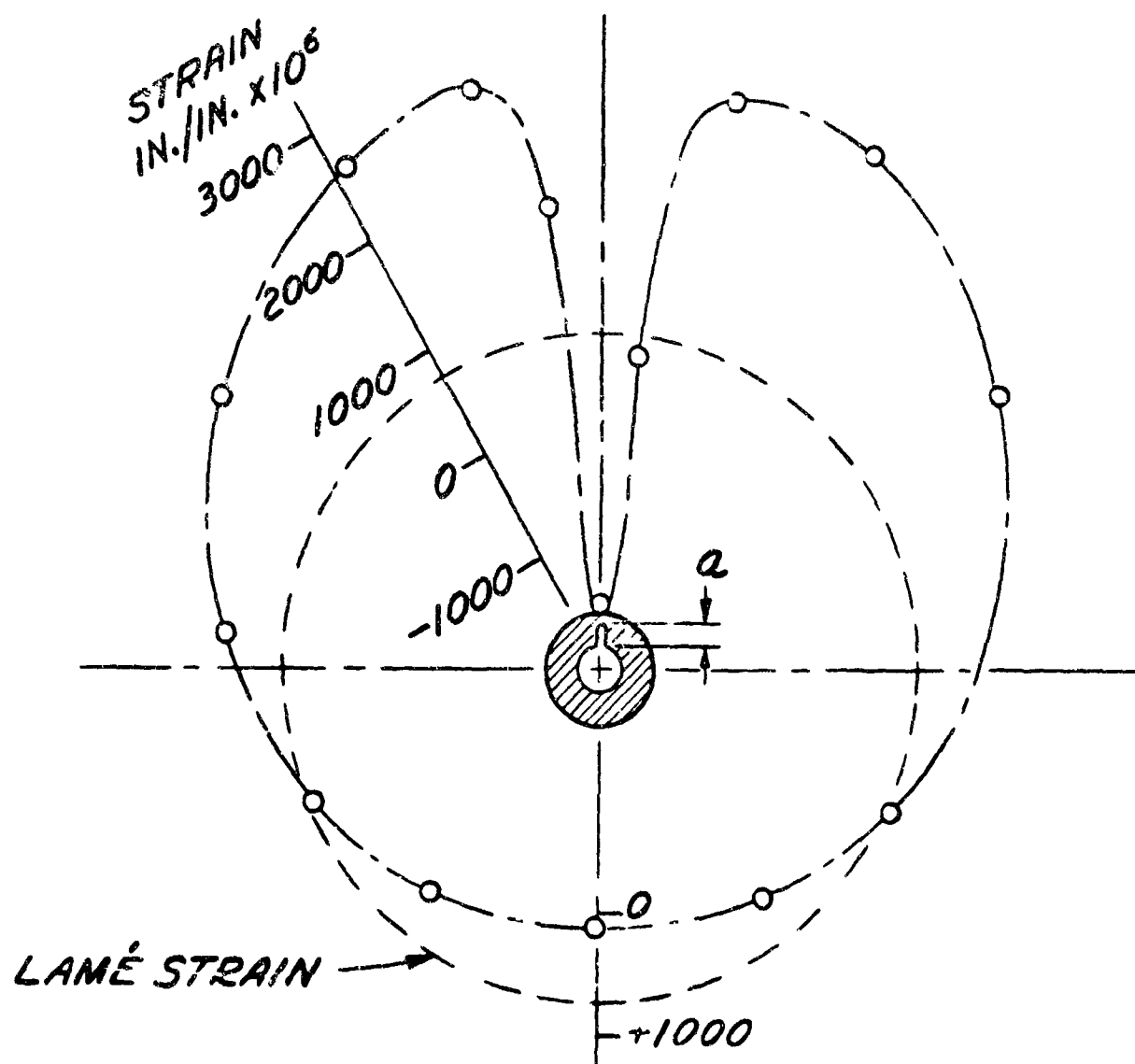
Figure 2. Compliance Test Set-up

Table I. Measured Tangential Strain at 10,000 psi Pressure

GAGE NO.	LOCATION Degrees	NOTCH LENGTH, in.									
		0	.043	.083	.117	.140	.152	.181	.189	.230	.316
1	0	240	220	145	80	5	- 10	- 90	-120	-375	-495
2	+ 7	230	230	180	145	85	95	90	—	235	450
3	- 7	240	225	160	100	105	30	- 20	- 5	- 40	100
4	+ 14	240	255	235	265	265	285	320	325	675	135
5	- 14	235	240	215	210	230	210	225	255	555	805
6	+ 29	240	265	310	360	405	420	470	495	760	840
7	- 29	240	265	300	340	400	400	455	485	780	875
8	+ 57	240	260	285	325	365	360	400	425	580	635
9	- 57	235	265	290	330	365	380	405	440	620	665
10	+ 86	220	250	260	280	295	285	295	320	395	405
11	- 86	230	255	225	285	—	—	315	—	—	—
12	+115	240	240	245	245	240	240	215	240	245	220
13	-115	240	250	240	255	250	250	240	255	—	250
14	+143	240	240	230	215	205	200	180	190	140	110
15	-143	240	240	—	220	205	215	190	205	155	120
16	±180	240	240	220	210	190	185	165	160	95	45

The gage positions shown are in degrees away from the point on the OD directly above the notch. A plot of the variation of strain around the tube for a deep notch and 30,000 psi pressure is shown in Fig. 3 compared with the uniform strain value for an uncracked cylinder at the same pressure⁽⁵⁾. The higher average strain in the tube due to the presence of the notch can be seen by a simple visual comparison of the two plots.

By careful numerical analysis of all the strain gage data, the change in outside volume of the cylinder, ΔV_o , and thus its compliance can be accurately determined as a function of notch length. Since the strain data is taken at the center of the 6 in. length of the cylinder, any end effects will have vanished and a plane strain analysis is appropriate.



$$a = 0.315$$

$$F = 30,000 \text{ PSI}$$

Figure 3. Measured Strain Distribution

NUMERICAL DATA ANALYSIS

By considering only a cross section of the cylinder through the strain gages, the numerical problem may be simplified and stated as follows. Given the tangential strain at selected points on the circumference of a circle, we wish to determine numerically the shape of the perimeter of the distorted figure and from this the increment in area. Lacking knowledge of the radial displacement, the problem is somewhat ambiguous. However, if we can interpolate the tangential strain measurements with an angular function and assume that the departure of the distorted perimeter from the original circle is small, then two simplified approaches suggest themselves.

First, we can integrate the tangential strain to obtain the change in length of the perimeter

$$\Delta P = \int_0^{2\pi} r \epsilon_{\theta}(\theta) d\theta ,$$

and assuming the distorted figure remains circular, the change in area enclosed by the perimeter is

$$\Delta A_0 = \frac{2P \Delta P + (\Delta P)^2}{4\pi}$$

As an alternative approach we can assume that any displacement of the perimeter is solely radial, that is

$$u_{\theta}(r_2, \theta) = 0$$

and then from

$$\epsilon(r_2, \theta) = \frac{1}{r_2} \frac{\partial u_{\theta}(r_2, \theta)}{\partial \theta} + \frac{u_r(r_2, \theta)}{r_2}$$

we have $u_r(r_2, \theta) = \epsilon_\theta(r_2, \theta) \cdot r_2$ and

$$\Delta A_0 = \int_0^{2\pi} \int_{r_2}^{r_2 + u_r(r_2, \theta)} r \, dr \, d\theta$$

Since these two approaches give reasonable bounds on the amount of distortion of a circular cross section, we can assume that the degree to which they approximate each other is an indication of the number of significant figures in our approximation of the increment in area.

Our choice of an angular function was an interpolating, periodic, cubic spline. This function was chosen on grounds of experience, intuition and personal interest; however, it does belong to the class of functions which approximate minimum strain energy and thus is a likely candidate for interpolating (or approximating) strain readings.

We give here a definition of a cubic spline. Those who are interested in the details of the construction and manipulation of such functions are referred to refs. 6-7.

Definition of a Cubic Spline

Given an interval $\alpha \leq x \leq \beta$,
a mesh on the interval

$$\Delta: \alpha = x_0 < x_1 < \dots < x_N = \beta,$$

and an associated set of ordinates

$$Y: y_0, y_1, \dots, y_N$$

then a cubic spline satisfies

$$S_\Delta(Y; x) \in C^2 \text{ on } [\alpha, \beta]$$

$$S_\Delta(Y; x_j) = y_j \quad (j = 0, 1, \dots, N)$$

and is coincident with a cubic on each subinterval

$$x_{j-1} \leq x \leq x_j \quad (j = 1, 2, \dots, N)$$

If in addition

$$S_{\Delta}^{(p)}(\alpha+) = S_{\Delta}^{(p)}(\beta-) \quad (p = 0, 1, 2)$$

the spline is said to be periodic with period $(\beta - \alpha)$.

If alternatively

$$S_{\Delta}(Y; x_j) = y_j + \epsilon_j \quad (j = 0, 1, \dots, N)$$

with the ϵ_j subject to some minimizing constraint, it is said to be an approximating rather than an interpolating spline.

As described in the previous section, the data was taken at 16 positions for 10 crack depths and 4 pressures. Of the 640 possible readings, 16 were missing because the tube ruptured before the last scheduled measurement, 35 were missing because of gage failure, 3 were apparent gage failures, and one was judged a transcription error. The last 39 were replaced by bi-quadratic interpolation.

To indicate the smooth nature of the strain data and interpolating functions and the obvious nature of the transcription error, we show fitted spline functions for four pressures at a crack depth of 0.117 inches, see Fig. 4. The datum at $+86^\circ$ and 30,000 psi looks like an outlier. It was recorded as $945 \mu \text{ in/in}$ and quite likely was really $845 \mu \text{ in/in}$, the value on the dashed curve in Fig. 4.

It is also apparent upon close examination of the data in Fig. 4 that the minimum strain is not at the indexed zero. Examination of the sectioned tube confirmed that the gages were, indeed, displaced a small positive angle from the true location of the simulated crack; however, this had no effect on the computation.

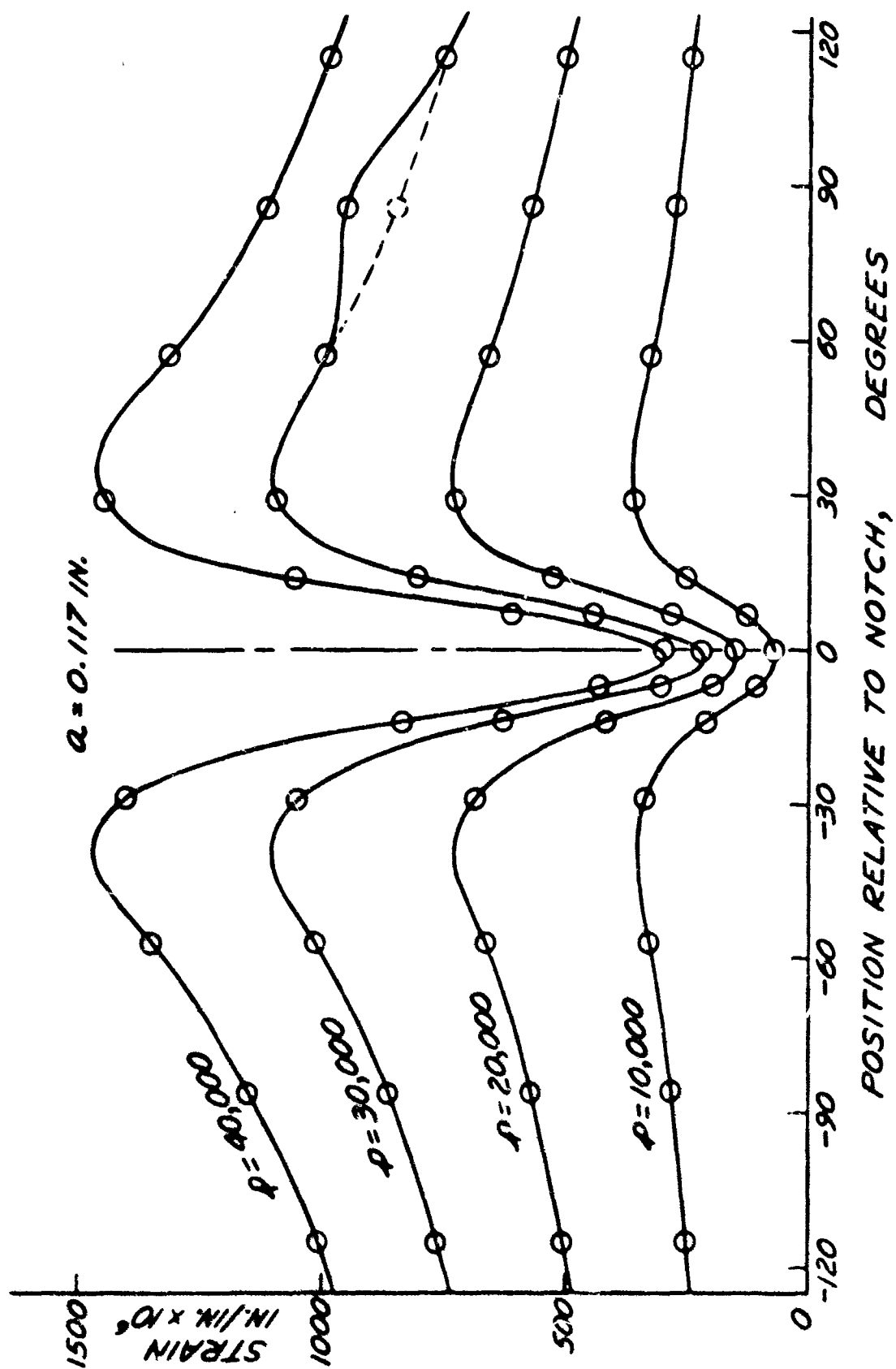


Figure 4. Numerical Strain Data

Evaluation of the change in area, ΔA_o , using the two methods described were found to agree with each other to four figures. These results are presented in Table II.

Table II. Change in Area Enclosed by the Outside Perimeter of the Cylinder

a, in.	ΔA_o , in. ²			
	at 10,000 psi	at 20,000 psi	at 30,000 psi	at 40,000 psi
0.0	0.001480	0.003009	0.004581	0.006157
0.043	0.001558	0.003130	0.004713	0.006193
0.083	0.001549	0.003126	0.004770	0.006371
0.117	0.001638	0.003315	0.005061	0.006663
0.140	0.001689	0.003452	0.005211	0.006957
0.152	0.001685	0.003446	0.005271	0.007023
0.181	0.001707	0.003559	0.005458	0.007289
0.189	0.001817	0.003682	0.005602	0.007436
0.280	0.002285	0.004610	0.007005	0.009555
0.316	0.002416	0.004939	0.007643	---

It was now desired to evaluate eq. (9) repeated below

$$K_I/p = \left[\frac{E}{2(1 - \nu^2)} \frac{d(\Delta V_o/p)}{da} \right]^{1/2} \quad (9)$$

where ΔV_o is the change in outside volume of the cylinder per unit length and thus is numerically equivalent to ΔA_o , and also

$$K_I^*/p = \left[\frac{E}{2(1 - \nu^2)} \frac{d(\Delta V_o/p)}{da^*} \right]^{1/2} \quad (10)$$

where $a^* = a + \frac{1}{2\pi} \left(\frac{K_I}{\sigma_y} \right)^2$ is an effective crack length suggested by Irwin⁽²⁾ to correct for effects of plastic deformation at the crack tip.

We also performed computations varying the correction by a constant, h,

$$a^* = a + \frac{h}{2\pi} \left(\frac{K_I}{\sigma_y} \right)^2 \quad (11)$$

to examine the effects of modifying the correction procedure.

To approximate $\Delta V_0(a)$ we used a non-periodic, approximating, cubic spline with an algorithm which minimized

$$\int_0^{a_n} \left\{ S''_{\Delta}(a) \right\}^2 da + \lambda \sum_{i=1}^n \left\{ S_{\Delta}(a_i) - \Delta v_{i-1} \right\}^2$$

where λ is introduced to allow us to strike a balance between the amount of smoothing desired versus our wish to respect the integrity of the data.

As a guide to the choice of λ we consider the type of K_I expression common for infinite bodies $K_I = (\text{constant}) a^{\frac{1}{2}}$ and see that

$$\frac{d^2 (K_I)}{da^2}$$

is strictly monotonic increasing. Thus, we want λ to be small enough so that this is also true of our approximating spline.

On the other hand we must of necessity evaluate a^* and K_I^*/p by an iterative process and λ must not be so small that this process is unstable. A value of $\lambda = 100$ proved to be a reasonable compromise leading to rapid and stable convergence of K_I^*/p .

RESULTS AND DISCUSSION

The K calibration results from the numerical analysis of the strain (eq. 9) are shown in Fig. 5. An ideal experiment and analysis would be expected to give results which all lie on the same curve. We believe that the main factor which accounts for the variation of the K_I/p curves is plastic deformation at the notch tip. Other factors, such as the finite notch width and thermal expansion of the cylinder due to pressure fluid heating, could affect the results. But plastic deformation is expected to occur most readily

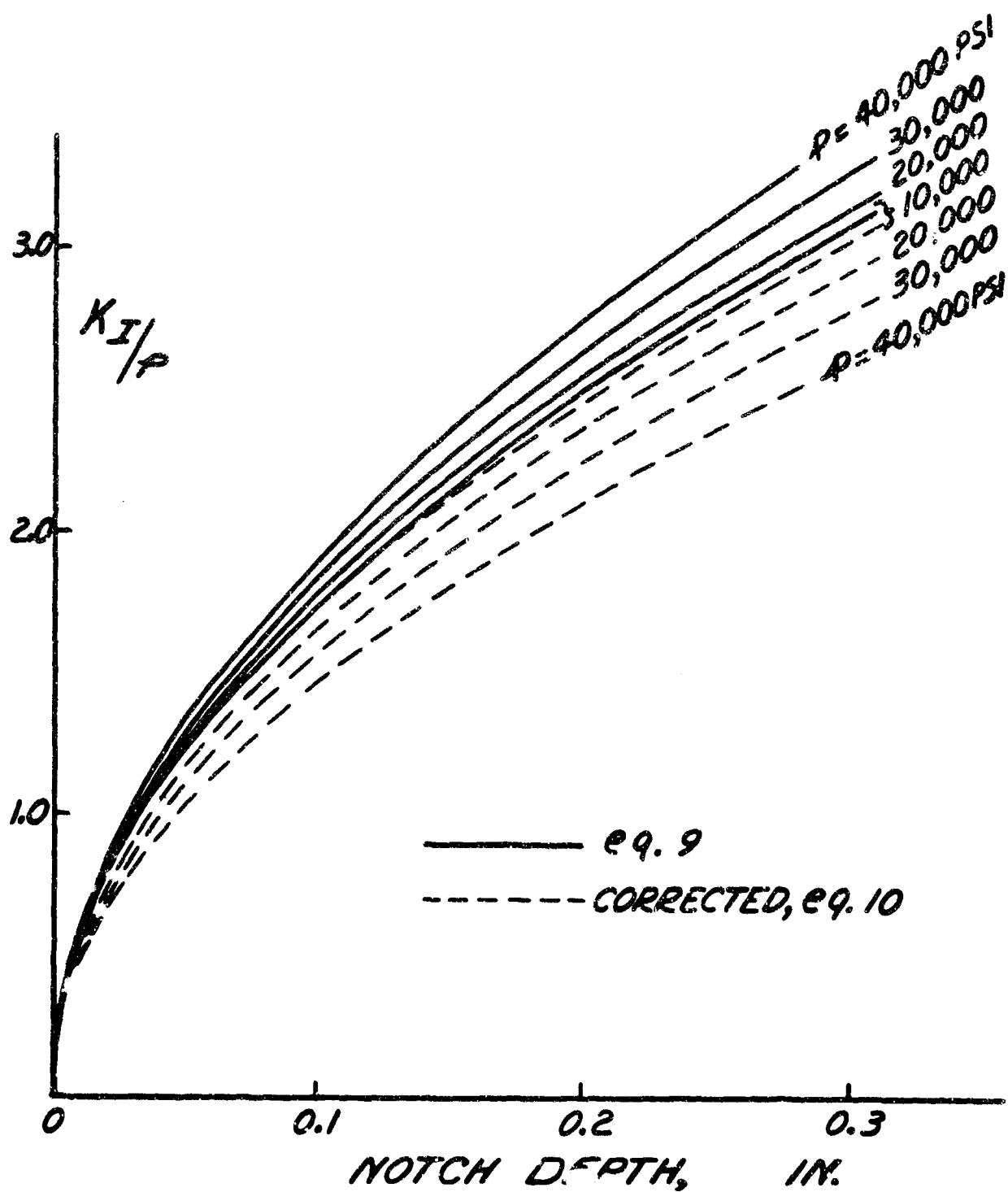


Figure 5. Compliance K Calibration Results

for combined high pressure and deep notches, the same conditions for which the variation of K_I/p is the greatest. Also, the strain readings taken at zero pressure after each run suggest that plastic deformation is occurring. The average residual strain for all readings through .181 in. notch depth is 3μ in/in., 8μ in/in. for the .189 reading, and 70μ in/in for the .280 in. readings. The tube fractured (at 38,500 psi) before the last pressure increment with a .316 in. notch present. The increase in residual strain and eventual fracture with increasing notch depth is a clear indication that significant plastic deformation was present in the cylinder for deep notches at high pressure.

The K results including the plastic zone correction of eq. (10) are shown as dashed curves in the figure. The large shift of the high pressure-deep notch results has little significance since the excessive plastic deformation probably present in these results makes a fracture mechanics analysis inappropriate. However, it is interesting to see in Fig. 6 that a smaller correction of $h = .3$ in eq. (11) causes all the deep notch data to fall on the same curve within 0.5%. This tends to support our belief that plastic deformation around the notch is the major uncertainty in the experiment and analysis.

The corrected 10,000 psi results from Fig. 5, considered to be the best, are repeated in Fig. 7 along with various analyses. Results are shown from Bowie's analysis⁽¹⁾ for a hole with a radial crack in an infinite plate under biaxial tension. As suggested in ref. (1), the plane-strain, plate solution can be used for an internally pressurized cylinder of infinite wall thickness with a radial crack if tensile load is replaced by pressure in the solution.

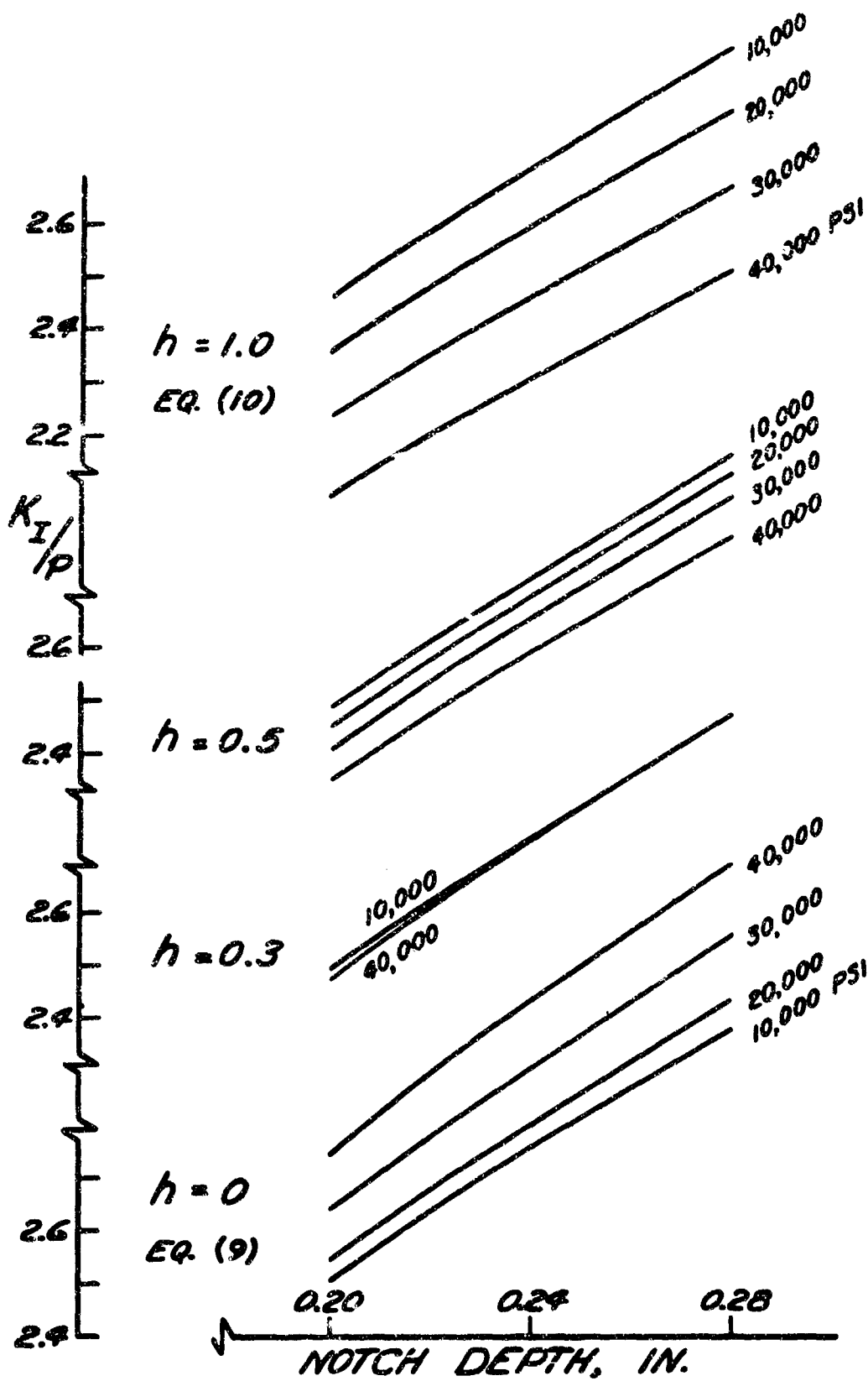


Figure 6. Variation of K with h

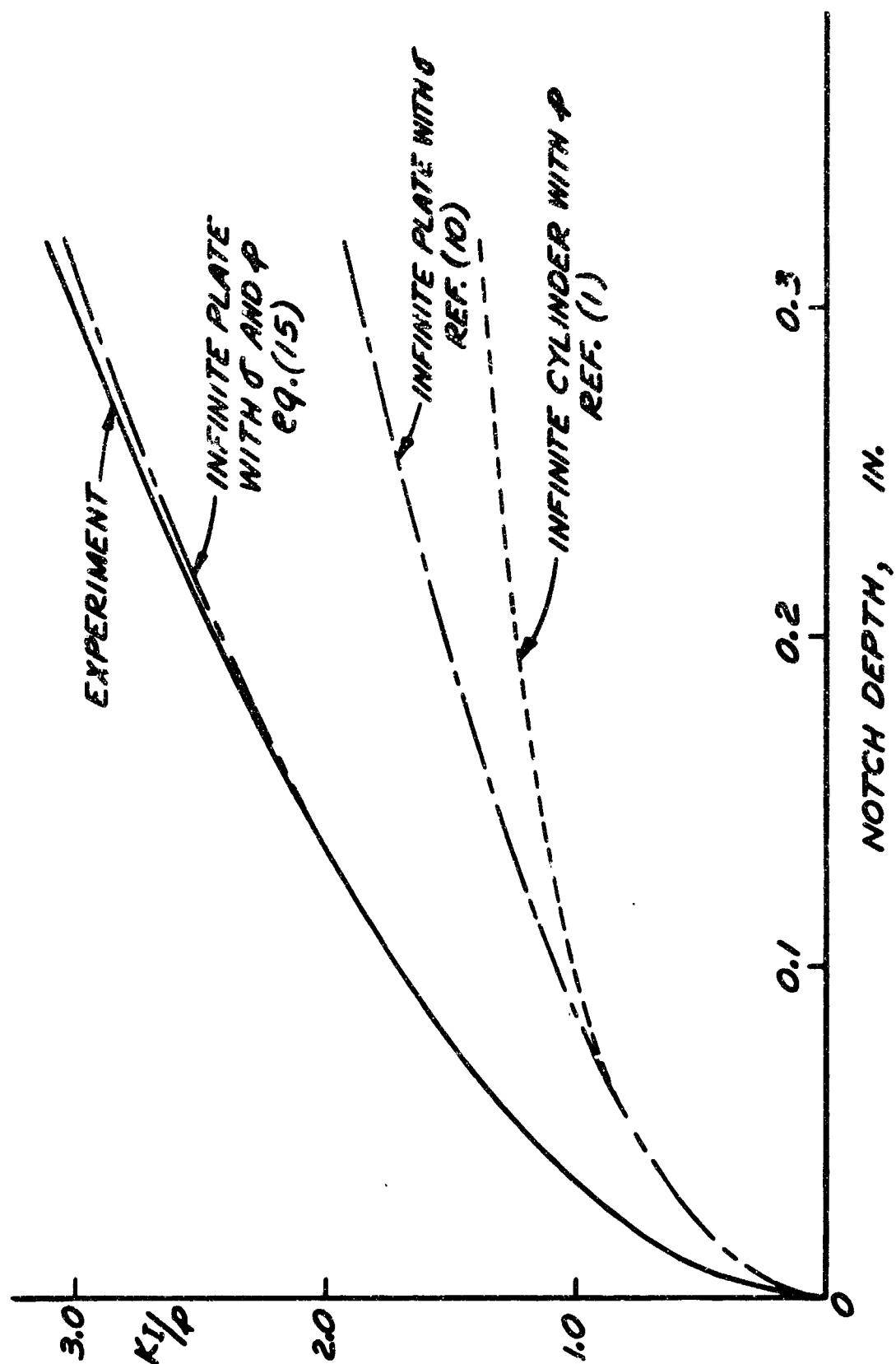


Figure 7. K Results from Experiment and Analysis

The resulting infinite cylinder K calibration coincides with the well-known semi-infinite plate solution⁽¹⁰⁾,

$$K_I = 1.12 \sigma \sqrt{\pi a} \quad (12)$$

for shallow notches, as would be expected. The semi-infinite plate solution is plotted in terms of pressure by using the Lamé relation⁽⁵⁾ between pressure and tangential stress in a cylinder.

$$\sigma_\theta = p \left[\frac{(r_2/r)^2 + 1}{(r_2/r_1)^2 - 1} \right] \quad (13)$$

where $r = r_1 + a$

The maximum value of σ_θ (corresponding to the ID) was used for plotting the plate solution, so the higher K_I/p values for deep notches are expected.

The K calibration for a pressurized cylinder should include the direct effect of pressure in the notch as well as the effect of the stresses in the cylinder which are present with no notch. Bueckner⁽¹¹⁾ obtained a solution for a pressurized notch in a half space,

$$K_I = 1.13 p \sqrt{\pi a} , \quad (14)$$

where the constant in the expression can be thought of as a free-surface correction factor applied to the solution for a pressurized notch in an infinite plate⁽¹²⁾. The superposition of the direct pressure effect, eq. (14), and the tangential stress effect using the maximum value of σ_θ , eqs. (12) and (13), results in

$$K_I = 3.06 p \sqrt{\pi a} . \quad (15)$$

The good agreement between the semi-infinite plate solution with combined pressure and stress and the experimental results is surprising, particularly for deep notches. It suggests that, if the experiment is to be believed, effects must be present in the experiment which reduce the expected increase in K_I for deep notches in a finite size specimen. The two dominant factors which lower the K_I of the cylinder are the drop off of tangential stress through the wall described by eq. (13) and the doubly connected nature of a hollow cylinder which tends to prevent bending in the wall.

Equation (16) is an attempt to account for these factors by including the decrease in σ_θ as a function of r and by including a bending-constraint expression which limits the increase in K_I for deep notches. Our choice for an expression to represent the bending constraint is the ratio of the K_I for a constrained-end, SEN plate(13) to the K_I for a semi-infinite plate.

$$K_I = \left[1.12 p \left\{ \frac{(r_2/r)^2 + 1}{(r_2/r_1)^2 - 1} \right\} \sqrt{\pi a} + 1.13 p \sqrt{\pi a} \right] \left[\frac{\overset{\text{finite plate,}}{\underset{\text{constrained ends,}}{K_I \text{ ref. (13)}}}}{\underset{\text{semi-infinite}}{K_I \text{ plate, eq. (12)}}} \right] \quad (16)$$

Of the two sets of results from ref. (13), we chose those for a plate of 2.6 length-to-width ratio as the better representation of the bending constraint in the test cylinder. Although the effects of σ_θ and bending constraint both change by as much as 50% for deep cracks, they counteract one another so that the net change is hardly noticeable. An expanded portion of the experimental results and values from eqs. (15) and (16) show just a few percent spread, see Fig. 8. So apparently, the smaller increase in K_I for deep notches in a cylinder with decreasing stress through the wall and bending constraint results in a K calibration for the test cylinder not much different from that of a semi-infinite plate.

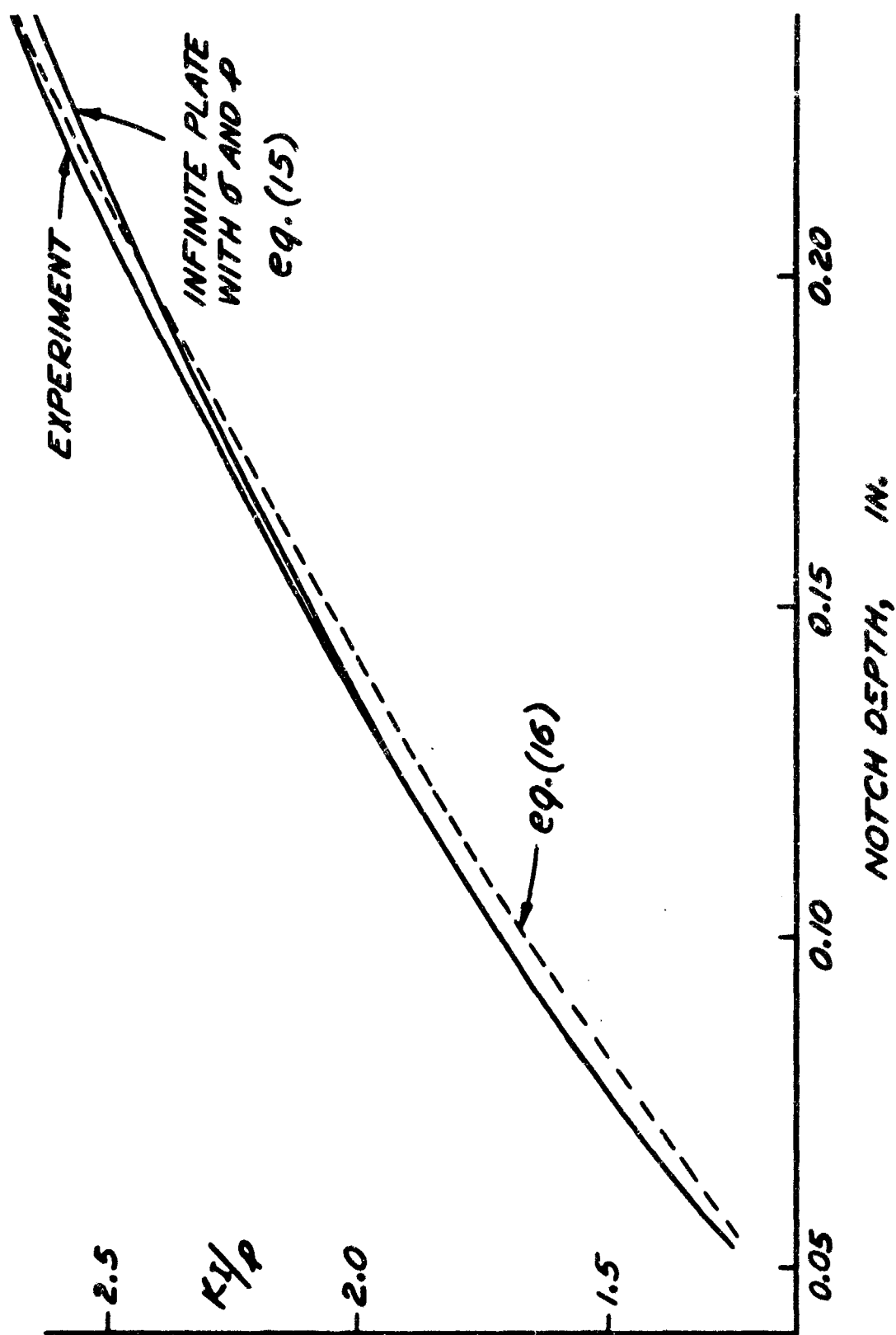


Figure 8. Comparison of K Results

It is difficult to comment on the accuracy of the experimental results since no solution is available for a direct comparison. Major effects due to notch-tip plasticity are probably avoided by using the low pressure data. The width of the notch is the other factor which could have a major effect on the results. The good agreement between the experimental K calibration for shallow notches and the infinite plate solution indicates that the notch width had no major effect since any effect should be at least as great for shallow notches. Finally, an indication that the experimental K calibration is not grossly in error is the K_I value calculated from the experimental curve of Fig. 7 for the 38,500 psi fracture pressure and .316 in. notch length. The value, 120,000 psi $\sqrt{\text{in.}}$, is near the critical value of K_I expected for the cylinder material.

Finally, it should be emphasized that the experimental K calibration shown in Fig. 7 strictly applies only to a cylinder of the dimensions given. However, we believe it can be extended to any cylinder with the same r_2/r_1 ratio by using the square-root size factor common to most K calibrations of finite specimens. Thus, a $K_I/p\sqrt{W}$ versus a/w plot of the results could be used for any cylinder of the same diameter ratio.

REFERENCES

- (1) O. L. Bowie, "Analysis of an Infinite Plate Containing Radial Cracks Originating at the Boundary of an Internal Circular Hole", Journal of Mathematics and Physics, Vol. 35, 1956, p.60-71
- (2) G. R. Irwin, "Structural Aspects of Brittle Fracture", Applied Materials Research, Vol. 3, April 1964, p.65-81
- (3) J. R. Rice, Private Communication, 1968
- (4) I. S. Sokolnikoff, Mathematical Theory of Elasticity, McGraw-Hill Book Company, New York, 1946, p.39-40
- (5) S. Timoshenko and J. N. Goodier, Theory of Elasticity, McGraw-Hill Book Company, New York, 1951
- (6) J. H. Ahlberg, E. N. Nilson and J. L. Walsh, The Theory of Splines and Their Applications, Academic Press, New York, 1967
- (7) G. Birkhoff and C. R. DeBoor, "Piecewise Polynomial Interpolation and Approximation", Approximation of Functions, H. L. Garabedian, ed., Elsevier, Amsterdam, 1965, p.164-190
- (8) T. N. E. Greville, ed., Theory and Applications of Spline Functions, Academic Press, New York, 1969
- (9) R. D. Scanlon, An Interpolating Cubic Spline Fortran Subroutine, Technical Report WVT-7010, Watervliet Arsenal, Watervliet, New York, 1969
- (10) L. A. Wigglesworth, "Stress Distribution in a Notched Plate", Mathematika, Vol. 4, 1957, p.76-96
- (11) H. F. Bueckner, "Some Stress Singularities and Their Computation by Means of Integral Equations", Boundary Problems in Differential Equations, R. E. Langer, ed., The University of Wisconsin Press, Madison, Wisconsin, 1960, p.216-230
- (12) G. C. Sih and H. Liebowitz, "Mathematical Theories of Brittle Fracture", Fracture, H. Liebowitz, ed., Academic Press, New York, 1968, Vol. II, p.67-190
- (13) O. L. Bowie and D. M. Neal, "Stress Intensity Factors for Single Edge Cracks in Rectangular Sheet With Constrained Ends", U. S. Army Materials Research Agency Technical Report 65-20, August 1965

Unclassified
Security Classification

DOCUMENT CONTROL DATA - R & D		
(Security classification of title, body of abstract and indexing annotation must be entered when the overall report is classified)		
1. ORIGINATING ACTIVITY (Corporate author)		2a. REPORT SECURITY CLASSIFICATION
Watervliet Arsenal Watervliet, N.Y. 12189		Unclassified
		2b. GROUP
3. REPORT TITLE		
A COMPLIANCE K CALIBRATION FOR A PRESSURIZED THICK-WALL CYLINDER WITH A RADIAL CRACK		
4. DESCRIPTIVE NOTES (Type of report and inclusive dates)		
Technical Report		
5. AUTHOR(S) (First name, middle initial, last name)		
John H. Underwood Ralph R. Lasselle and Moayyed A. Hussain Raymond D. Scanlon		
6. REPORT DATE	7a. TOTAL NO. OF PAGES	7b. NO. OF REFS
May 1970	34	13
8a. CONTRACT OR GRANT NO.	8b. ORIGINATOR'S REPORT NUMBER(S)	
AMCMS No. 501B.11.85500 A. PROJECT NO. DA Project No. 1T061102B32A C.	WVT-7026	
4.	9b. OTHER REPORT NO(S) (Any other numbers that may be assigned this report)	
10. DISTRIBUTION STATEMENT		
This document has been approved for public release and sale; its distribution is unlimited.		
11. SUPPLEMENTARY NOTES		12. SPONSORING MILITARY ACTIVITY
		U.S. Army Weapons Command
13. ABSTRACT		
<p>The K calibration for an internally pressurized, thick-wall cylinder with a straight, radial notch has been determined from a compliance test. The method suggested by Irwin is used with compliance defined as the change in internal volume of a cylinder divided by applied hydrostatic pressure rather than the usual load-elongation definition. The derivative of internal volume change with respect to notch depth, "a", is obtained by numerical analysis of tangential strain measurements on the OD of the test cylinder. This derivative leads directly to the K calibration for the cylinder. Cubic spline functions are used to approximate both the strain as a function of position on the cylinder and the resulting volume change as a function of "a". Also included in the determination of K is a proof, using the divergence theorem in the theory of elasticity, that the derivatives with respect to "a" of internal and external volume change are identical. This allows the use of external strain measurements to determine K based on internal volume change.</p> <p>The compliance K calibration nearly coincides with a semi-infinite plate solution simulating both the tangential stress due to pressure and the direct effect of pressure in the notch, $K_1 = 1.12 \sqrt{a} + 1.13 \sqrt{a}$. This unexpected agreement, particularly for values of a/w up to 0.6, is explained by the combination of bending constraint and drop off of tangential stress in the cylinder wall.</p>		

DD FORM 1473

REPLACES DD FORM 1473, 1 JAN 64, WHICH IS OBSOLETE FOR ARMY USE.

Unclassified

Security Classification

Unclassified

Security Classification

14. KEY WORDS	LINK A		LINK B		LINK C	
	ROLE	WT	ROLE	WT	ROLE	WT
Fracture Mechanics						
Stress Intensity Factor						
Compliance Test						
Cubic Spline Functions						
Divergence Theorem						

Unclassified

Security Classification